Pergamon

Int. J. Heat Mass Transfer. Vol. 40, No. 17, pp. 4209–4218, 1997

Printed in Great Britain
0017–9310/97 $17.00+0.00

PII: S0017–9310(97)00035–5

Pulsating flow and heat transfer in a pipe partially filled with a porous medium

ZHIXIONG GUO, SEO YOUNG KIM and HYUNG JIN SUNG†

Department of Mechanical Engineering, Korea Advanced Institute of Science and Technology, Yusong, Taejon, 305-701, Korea

(*Received* 11 *January* 1996 *and in final form* 19 *November* 1996)

Abstract—A numerical study is made of pulsating flow and heat transfer characteristics in a circular pipe partially filled with a porous medium. The Brinkman–Forchheimer-extended Darcy model is adopted for the porous matrix region, which is attached to the pipe wall. The impacts of the Darcy number Da, the thickness of porous layer S, the ratio of effective thermal conductivity of porous material to fluid, R_k, as well as the pulsating frequency, β, and the amplitude, A, are investigated. The enhanced longitudinal heat conduction due to pulsating flow and the enhanced convective heat transfer from high conducting porous material are examined. The maximum effective thermal diffusivity is found at a critical thickness of porous layer. The effects of pulsating amplitude and frequency on heat transfer are also scrutinized. © 1997 Elsevier Science Ltd.

1. INTRODUCTION

It is generally known that heat transfer can be enhanced by using saturated porous media in a forced convective fluid flow system [1–5]. Technological applications can be found in thermal insulation, heat exchangers, geothermal reservoirs and nuclear waste repositories, to name but a few. However, if a full porous media system fills a confined passageway, the penalty is the significant pressure drop due to the porous material. Forced convection in a composite system, in which a fluid-saturated porous material occupies only a part of the passage, has been the topic of several investigations published in the literature since the work of Poulikakos and Kazmierczak [6]. An important finding was made by Tong and Sharachandra [5] that the use of only a slice of porous material inserted in a channel could give rise to considerably augmentation of convective heat transfer. An enhanced heat transfer in an annular duct partially filled with a porous medium with high permeability and conductivity, was observed in a recent analytical solution of Chikh *et al.* [7] with the Brinkman model. Sung *et al.* [8] simulated numerically the forced convection from an isolated heat source in a channel, in which the loss of pressure drop was reduced by employing a partially-porous channel.

On the other hand, much attention has been given to both convective and conductive heat transfers by superimposing pulsation on the mean flow in a confined passageway. The motivation stems from a better understanding of a host of thermal engineering applications, e.g. in ducts, manifolds and Stirling engines. It has been broadly recognized that pulsation produces an enhanced axial diffusion in the presence of an axial gradient in concentration or temperature [9–12]. The enhanced thermal diffusion can be thousands of times larger than the transport by axial molecular conduction [11, 12].

As pointed out by Simon and Seume [13], however, studies of pulsating flow and heat transfer through a porous medium are relatively scarce and often incomplete. Recently, Kim *et al.* [14] simulated the pulsating flow and heat transfer in a channel filled with a porous medium. Khodadadi [15] treated analytically an oscillatory flow through a porous medium channel bounded by two impermeable parallel plates. However, in view of pressure drop and axial thermal diffusion, it is expected that a more effective enhanced heat transfer may be achieved by pulsating flow through a pipe partially filled with a porous medium. The present issue addresses this problem. Some promising thermal engineering applications pertaining to the present investigation are exemplified by advanced heat exchangers, regenerators and Stirling engines. The main motivation of the present study is to see the effects of both the heat transfer enhancement factor by the presence of pulsating flow and the adoption of partial porous medium in order to reduce the mechanical loss due to pressure drop. In addition, a literature survey reveals that no published accounts are available which involve the present aspect.

In the present treatise, the Brinkman–Forchheimer-extended Darcy model is employed for the region of porous medium. Efforts are focused on identifying the influence of non-dimensional parameters on heat transfer properties, such as the Darcy number, the thickness of porous layer, the ratio of effective thermal conductivity of the porous material to fluid thermal

† Author to whom correspondence should be addressed.

NOMENCLATURE

a	pipe radius	s, S	dimensional, non-dimensional thickness of porous layer
A	amplitude of pressure gradient pulsation	t	non-dimensional time
A_U	amplitude of velocity pulsation	T	dimensional temperature
B	non-pulsating part of pressure drop	u, U	dimensional, non-dimensional velocity
C_F	inertia coefficient of porous medium	$\bar{u}_s$	space-averaged steady velocity.
C_p	specific heat capacity of fluid	Greek symbols	
Da	Darcy number, K/a^2	α	thermal diffusivity of fluid
f	frequency of pulsation	β	Womersley number, $a\sqrt{2\pi f/\nu}$
k	thermal conductivity of fluid	ε	porosity of porous medium
K	permeability of porous medium	ν	kinematic viscosity
Nu	Nusselt number, $2/(\Theta_w-\Theta_b)$	ϕ	phase lead (lag)
p, P	pressure, non-dimensional pressure	ρ	density
Pr	Prandtl number	τ	dimensional time
q''	heat flux	Θ	non-dimensional temperature
r, x	dimensional coordinates	ΔX	non-dimensional tidal displacement.
R, X	non-dimensional coordinates	Subscripts	
R_c	ratio of heat capacity of porous medium to fluid	b	bulk
R_k	ratio of thermal conductivity of porous medium to fluid	eff	effective value of porous medium
R_{eff}	ratio of effective thermal diffusivity due to pulsation	s	steady component
Re	Reynolds number, $2a\bar{u}_s/\nu$	w	wall.

conductivity, the frequency and the amplitude of pulsation.

2. MATHEMATICAL FORMULATION

The specific configuration of flow and heat transfer in a circular pipe partially filled with a porous medium is sketched in Fig. 1. Under the assumptions: (1) the porous medium is homogeneous, isotropic and in local equilibrium with the fluid; (2) the thermophysical properties of the fluid and the effective properties of the porous medium are constant; (3) the axial conduction effect in the energy equation is negligible, a single set of the governing equations, with the Brinkman–Forchheimer-extended Darcy model in dimensionless form, can be written as

$$\frac{\partial U}{\partial t} = -\frac{\partial P}{\partial X} + \frac{2}{Re}\frac{1}{R}\frac{\partial}{\partial R}\left(R\frac{\partial U}{\partial R}\right) - \zeta\left[\frac{2\varepsilon}{DaRe} + \frac{\varepsilon^2 C_F}{\sqrt{Da}}|U|\right]U, \quad (1)$$

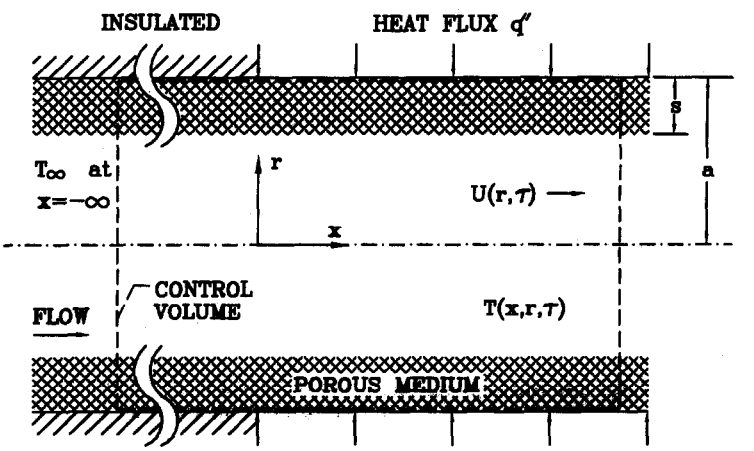

Fig. 1. Schematic diagram of heated circular pipe partially filled with a porous medium.

$$R_c\frac{\partial\Theta}{\partial t}+U\frac{\partial\Theta}{\partial X}=\frac{2[1+(R_k-1)\zeta]}{\varepsilon RePrR}\frac{\partial}{\partial R}\left(R\frac{\partial\Theta}{\partial R}\right) \quad (2)$$

in which U represents the fluid velocity in the fluid region as well as the Darcian velocity in the porous medium portion. The above formulations are applicable to both fluid and porous regions; the fluid-occupied region is identified by setting the index $\zeta = 0$ and the porous region tagged by $\zeta = 1$. It is remarked that the one-equation approach with a harmonic mean formulation may not yield correct results in conventional finite-difference treatment. However, by using a control-volume based method, such as the one employed here, the interface matching conditions are satisfactorily taken care of [16]. The justification of this approach has been thoroughly checked in the preparation stage [17, 18]. The porous medium is attached to the wall of the pipe and its non-dimensional thickness is $S = s/a$. In the present paper, the porosity ε of the porous medium is set to be 0.6 and the inertia coefficient C_F in Forchheimer's extension is taken to be equal to 0.057 in accordance with the previous works [14, 15], which generally addressed applications in advanced heat exchangers and regenerators. While the precise value of ν_{eff} in Brinkman's extension remains unclear, it is taken to be the same as ν, as a first approximation, as ascertained by Lundgren [19].

In the above, the non-dimensional variables are defined as

$$X=\frac{x}{a},\quad R=\frac{r}{a},\quad U=\frac{u}{\varepsilon\bar{u}_s},\quad t=\frac{\tau}{a/\bar{u}_s},$$

$$P=\frac{p}{\rho\bar{u}_s^2},\quad \Theta=\frac{T}{q''a/k},\quad Re=\frac{2a\bar{u}_s}{\nu},\quad Pr=\frac{\nu}{\alpha},$$

$$Da=\frac{K}{a^2},\quad R_k=\frac{k_{\text{eff}}}{k},\quad R_c=\frac{(\rho C_p)_{\text{eff}}}{\varepsilon(\rho C_p)} \quad (3)$$

where Re stands for the Reynolds number, Pr the Prandtl number, Da the Darcy number, R_k the thermal conductivity ratio and R_c the heat capacity ratio, respectively. The space-averaged steady state velocity is represented by $\bar{u}_s$.

The pulsating pressure gradient is given as

$$-\frac{\partial P}{\partial X}=-\left(\frac{\partial P}{\partial X}\right)_s\left[1+A\sin\left(\frac{2\beta^2}{Re}t\right)\right] \quad (4)$$

where the time-averaged non-dimensional pressure drop is denoted by $B \equiv -(\partial P/\partial X)_s$ and A is the amplitude of pulsation. The Womersley number β is defined as $\beta = a\sqrt{2\pi f/\nu}$, where f is the pulsating frequency. The boundary conditions are as follows:

$$\frac{dU}{dR}=0,\quad \frac{\partial\Theta}{\partial R}=0,\quad \text{at } R=0$$

$$U=0,\quad \frac{\partial\Theta}{\partial R}=\frac{1}{R_k},\quad \text{at } R=1. \quad (5)$$

To solve the above system of equations, Chatwin's approximation is employed [9], i.e.

$$\frac{\partial\Theta}{\partial X}=\frac{4}{RePr}=\text{constant}. \quad (6)$$

3. NUMERICAL SCHEME

The fully implicit scheme based on the control-volume formulation [16] was introduced to discretize the governing equations. A harmonic-mean formulation was adopted for the interface diffusion coefficients between two control volumes, and this approach is capable of handling abrupt changes in these coefficients at the fluid/porous interface. The resulting algebraic equations were solved by the tridiagonal matrix algorithm. In the radial direction, non-uniform grid points were densely packed near the pipe wall and the fluid/porous interface to resolve abrupt changes of velocity and temperature in these regions. The number of mesh points was 100. To ensure sufficient temporal resolution, 3600 time intervals were utilized to constitute one pulsating cycle for higher frequencies, whereas 360 time steps for lower frequencies. The temporally periodic solution was attained usually after 10 cycles of pulsation.

In actual calculations, a solution for the steady non-pulsating flow was adopted as the initial state condition. Several trial calculations were repeated to test the sensitivity of the results to grid size and time interval. The outcome of these exercises was satisfactory. The Reynolds number was set to be 50, the Prandtl number 7.0 and the ratio R_c 1.0 in the present computation.

4. RESULTS AND DISCUSSION

The character of pulsating flow is marked by the two prime non-dimensional parameters, i.e. the pulsation frequency β and the amplitude A. In the case of a pipe partially filled with a porous medium, the Darcy number Da, the thickness of porous material S and the ratio R_k are also essential ingredients. The present paper focuses on the influence of the above parameters on fluid flow and heat transport. The calculation domain is set as $0.1 \leqslant \beta \leqslant 10$, $0 \leqslant A \leqslant 2.0$, $0 \leqslant S \leqslant 1.0$, $10^{-2} \leqslant Da \leqslant 10^{-1}$ and $1.0 \leqslant R_k \leqslant 100$.

To ascertain the reliability and accuracy of the present simulation, a comparative example of non-pulsating velocity profiles is displayed in Fig. 2. It corresponds to the case where the thickness of porous medium near the wall equals 20% of the pipe radius ($S = 0.2$). The pressure drop remains constant ($B = 0.32$). In accordance with the analysis [6], the Forchheimer term of porous material is not accounted for ($C_F = 0$). It is seen that the present numerical results are in excellent agreement with the analytical solutions of Poulikakos and Kazmierczak [6]. This exemplifies the reliability of the present simulation.

Based on the pulsating pressure gradient in equa-

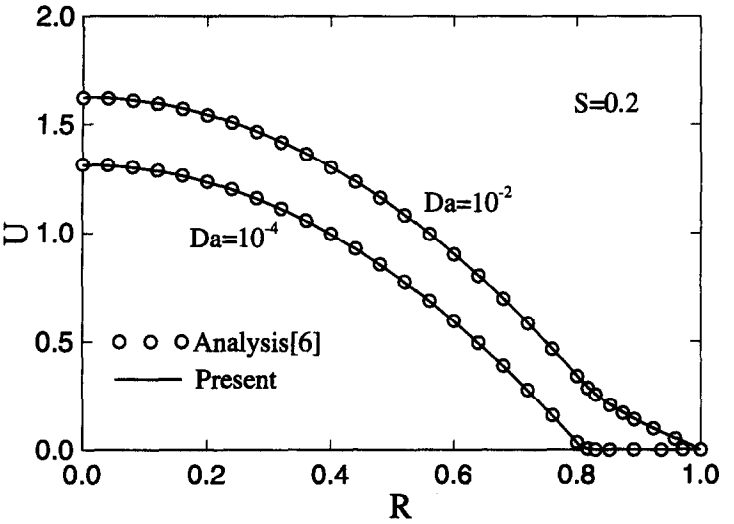

Fig. 2. Comparison of steady non-pulsating velocity profile. $S = 0.2$, $B = 0.32$.

tion (4), the fluctuating part of velocity in the fluid region can be obtained in a manner similar to the previous development [21].

$$U - U_s = A_U \sin\left(\frac{2\beta^2}{Re}t + \phi\right) \tag{7}$$

where U_s represents the steady component of local velocity in the cross-section of the pipe. A_U stands for the amplitude of fluctuating part of velocity and ϕ is the phase lag as compared with the pressure gradient pulsation. In the porous region, since C_F is very small ($C_F = 0.057$), the non-linearity of the velocity field is very weak. Accordingly, the fluctuating velocity field can be approximately described in the form of equation (7).

The time-dependent fluctuating velocity profiles during one pulsation cycle are displayed in Fig. 3(a), where the conditions are $Da = 10^{-4}$, $S = 0.2$, $A = 0.9$ and $\beta = 10$. The part of porous portion ($S = 0.2$) is enlarged in Fig. 3(b). It can be seen that the profiles in the porous region are similar to the case filled with full porous matrix, whereas the profiles in the fluid region are almost equivalent to those of no porous media. For a further discussion on the structure of the fluctuating velocity, the amplitude profiles of the fluctuating velocity component are exhibited in Fig. 4(a). The conditions are as follows: $Da = 10^{-2}$ or 10^{-4}, $\beta = 1$ or 10. The phase lag profiles are shown in Fig. 4(b). From the enlarged view of the inset of Fig. 4(a), it is found that the effect of β on the fluctuating

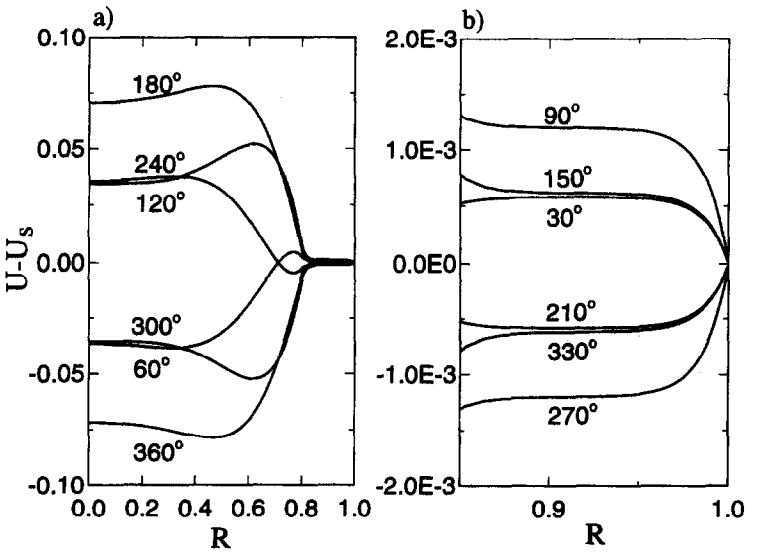

Fig. 3. Pulsating part of velocity distribution. $A = 0.9$, $\beta = 10$, $Da = 10^{-4}$ and $S = 0.2$: (a) overall; (b) near the wall.

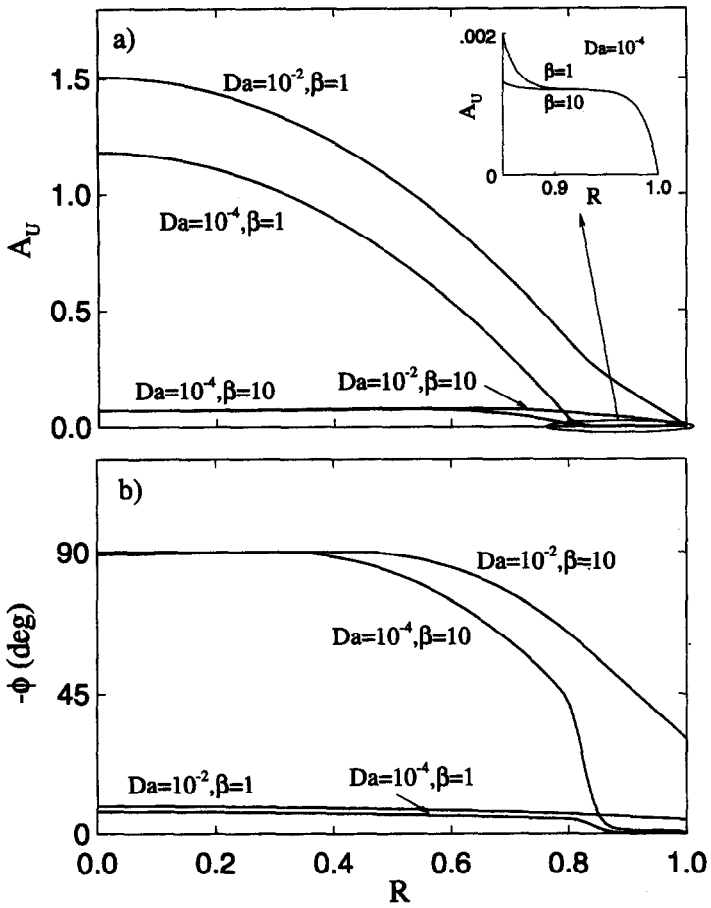

Fig. 4. (a) Amplitude and (b) phase lag of pulsating part of velocity for diverse Da and β: $A = 0.9$, $B = 0.32$, $S = 0.2$.

velocity amplitude profiles is negligible in the porous region when Da is small as 10^{-4}. This trend is in accordance with the result of Kim *et al.* [14] in the case of pulsating flow through a channel filled with a full porous medium. In the fluid region, the fluctuating amplitude profiles are shown to be strongly dependent on β and Da. Of much interest is that, when β is high ($\beta = 10$), Da has little influence on the fluctuating amplitude and its profile is flat in most areas of the region. When β is relatively low ($\beta = 1$), however, the amplitude profile is similar to the case of the non-pulsating flow as shown in Fig. 2. Due to the resistance of porous medium to the fluid flow, the phase delay between the fluid and porous regions in pulsating flow is originated. The magnitude of the phase lag increases as both Da and β increase. The velocity in the fluid region begins to lag behind the pressure drop about 90° for $\beta = 10$, and the variation is consistent with the previous works of Uchida [20] and Siegel and Perlmutter [22]. The phase lag in the porous region decreases dramatically. In particular, the velocity is nearly in phase with the fluctuating pressure drop when Da is small ($Da = 10^{-4}$) [15].

In designing heat exchangers or regenerators, the primary goal is to minimize the mechanical loss due to pressure drop and to enhance the heat transfer rate from and to the working fluid. It is, therefore, important for the designer to compromise the trade-off between pressure drop and heat transfer. One major motivation of the present work is to reduce pressure drop by employing a pipe partially filled with a porous medium instead of full porous medium. In an effort to demonstrate the characteristics of the pressure drop B against Da and S, the variation of B is depicted in Fig. 5. The other conditions are fixed at $Re = 50$, $\varepsilon = 0.6$ and $C_F = 0.057$. It is seen that, as S increases or Da decreases, B increases. This means that the resistance of porous matrix to the flow becomes large, as Da decreases or S increases. Special attention is given to case ($Da = 10^{-4}$), the pressure drop (B) is substantially increased, i.e. $B = 248$ at $S = 1$. This can be compared with $B = 0.32$ at $S = 0$. However, when $S \leqslant 0.5$, the pressure drop is mildly affected by Da.

Next, the influence of partial porous medium S on heat transfer enhancement is examined. The Nusselt number is plotted in Fig. 6 against the porous layer thickness ($0 \leqslant S \leqslant 1$), and the effective thermal conductivity ratio ($R_k = 1, 10$ and 100). Two cases of permeability are also selected for comparison:

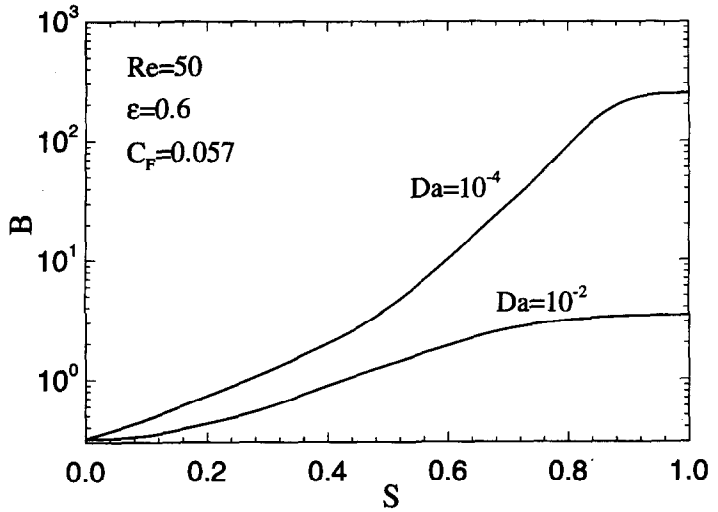

Fig. 5. Non-pulsation pressure drop as a function of the thickness of porous layer.

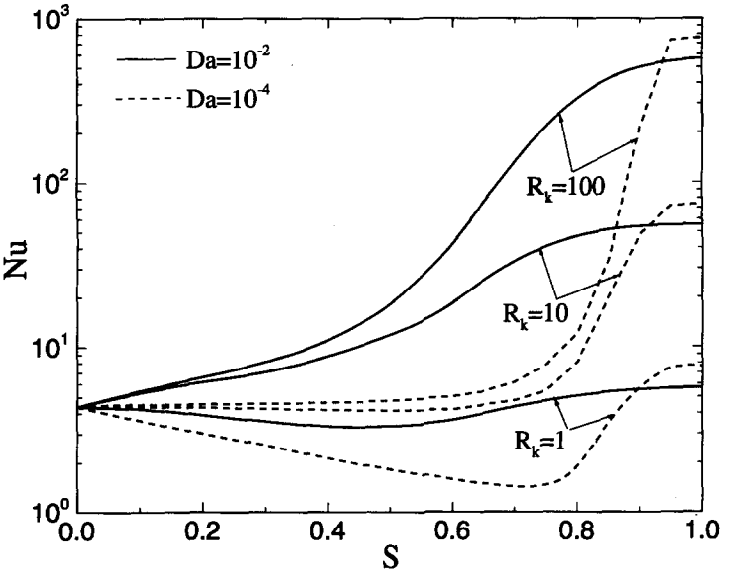

Fig. 6. Variations of *Nu* number as a function of the thickness of porous layer.

$Da = 10^{-2}$ and 10^{-4}. As seen in Fig. 6, the dependence of *Nu* on *S* is not straightforward. For a higher thermal conductivity porous material ($R_k = 100$), the Nusselt number increases monotonically with increasing *S*. However, for a lower value of R_k ($R_k = 1$), a minimum exists in the *Nu* distributions. When $S \geqslant 0.9$, *Nu* increases considerably up to a nearly constant value. These findings are qualitatively in conformity with the analysis of an annular duct partially filled with a porous medium by Chikh *et al.* [7]. It is also worth noting that the dependence of *Nu* on *Da* is significant.

The impact of pulsation on the heat transfer in a pipe partially filled with a porous medium is inspected in the following. In analyzing the heat transfer enhancement due to pulsation, difficulties arise in defining the time-dependent bulk temperature or the Nusselt number over a cycle. It is found in the literature that many versions of the Nusselt number were devised to account for their results [21–24]. The arguments regarding the inconclusive unsteady Nusselt number usage can be found in several studies [21, 23, 24]. Thus, in the present study of pulsating flow in a pipe, the effective axial thermal diffusion due to pulsation is adopted to avoid these confusions. Several other researchers adopted this concept to clarify the characteristics of oscillatory flow heat transfer [10–12]. The physical mechanism of the enhanced heat conduction in oscillatory flows within a confined passageway can be applied to the enhanced axial heat diffusion due to pulsation [10, 11]. This is based on the fact that large oscillating temperature gradients in the direction normal to the wall are produced and an axial temperature gradient is present.

In the present issue, efforts are focused on identifying the influence of non-dimensional parameters on

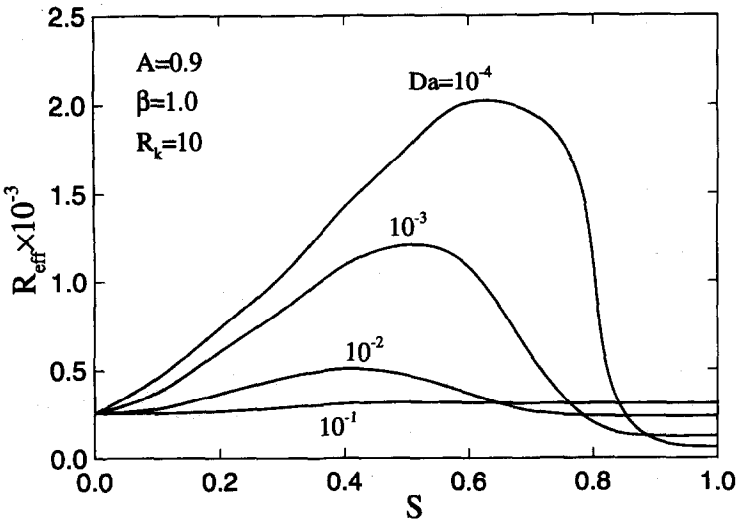

Fig. 7. Variations of R_{eff} against the thickness of porous layer for $10^{-4} \leqslant Da \leqslant 10^{-1}$. $A = 0.9$, $\beta = 1.0$, $Pr = 7.0$, $Re = 50$ and $R_k = 10$.

the effective thermal diffusivity $\alpha(1 + R_{eff})$. R_{eff} denotes the ratio of the effective thermal diffusivity due to pulsation, which can be expressed as

$$R_{eff} = \Delta\Theta_w (RePr)^2/8 \tag{8}$$

where $\Delta\Theta_w$ is the increment of wall temperature due to pulsation. This can be derived by taking heat balance on the control volume shown in Fig. 1. The final form of $\Delta\Theta_w$ is

$$\Delta\Theta_w = \frac{-\int_0^{1/f}\int_0^1 (\Theta-\Theta_s)(U-U_s)R\,dR\,d\tau}{\int_0^{1/f}\int_0^1 U_s R\,dR\,d\tau}. \tag{9}$$

Here, the subscript s stands for the steady-state.

The variations of R_{eff} against the porous layer thickness S are illustrated in Fig. 7 for several Darcy numbers ($10^{-4} \leqslant Da \leqslant 10^{-1}$). The other conditions are set as $A = 0.9$, $\beta = 1.0$, $Pr = 7.0$, $Re = 50$ and $R_k = 10$. As seen in Fig. 7, the dependence of R_{eff} on S is non-monotonic. The heat transfer in a pipe partially filled with porous media is rather augmented than that fully filled with porous media ($S = 1$). As mentioned earlier, the above-stated partial filling of porous media is desirable in reducing the mechanical loss due to pressure drop. An optimal value of S can be obtained in Fig. 7, which causes a lower mechanical loss ($S < 1.0$) and a larger heat transfer rate. These phenomena can be explained from the definition of $\Delta\Theta_w$ in equation (9) that R_{eff} is proportional to the integration of the product in two terms, ie $(\Theta-\Theta_s)(U-U_s)$. The two terms, $\Theta-\Theta_s$ and $U-U_s$ represent the fluctuating temperature and the fluctuating velocity due to pulsation, respectively. As S increases, the velocity and the attendant temperature profiles in the cross-section deviate further away from those of the non-pulsation state. These deviations give rise to the increase of the transverse integration in the cross-section. Consequently, R_{eff} increases. However, after reaching the maximum value of R_{eff}, the adverse effect occurs, i.e. the transverse integration of the product of two terms decreases as S increases. The influence of Da on R_{eff} is also substantial. As Da increases, the dependence of R_{eff} on S weakens considerably. Another finding in Fig. 7 is that the peak of R_{eff} shifts towards the larger values of S with decreasing Da. However, as S increases further, near the region $0.7 \leqslant S \leqslant 1.0$, the dependence of R_{eff} on Da is shown to be different from that of the preceding ones. In particular, around $S = 0.8$, the R_{eff} distribution by Da is entirely exceptional. This peculiar phenomenon will be recapitulated in Fig. 8. Furthermore, when $S \geqslant 0.9$, R_{eff} decreases as Da decreases.

Discussion is extended to the effects of Da and S on R_{eff} in Fig. 8. It is found that, when Da is larger than a critical value ($Da > 0.02$), the influence of S on R_{eff} tends to be small. This is caused by the fact that the resistance of porous matrix to flow is so low that the porous thickness gives little influence on the velocity profiles. When S is smaller than $S \approx 0.5$, R_{eff} increases monotonically as Da decreases. However, as anticipated in Fig. 7, a drastically different picture emerges on the distribution of R_{eff} when S is larger than $S \approx 0.6$. In particular, the dependence of R_{eff} on Da is marginal for $S \approx 0.8$. Finally, R_{eff} decreases as Da decreases in the case of $S = 1.0$.

When dealing with time-dependent pulsating flows, it is convenient to introduce the concept of tidal displacement ΔX [11]. This quantity can be defined as the cross-section averaged maximum axial distance, which the fluid elements travel during one half period of the pulsation. Mathematically the non-dimensional tidal displacement equals

$$\Delta X = \frac{1}{2}\int_0^{1/f}\int_0^1 |(U-U_s)|R\,dR\,d\tau. \tag{10}$$

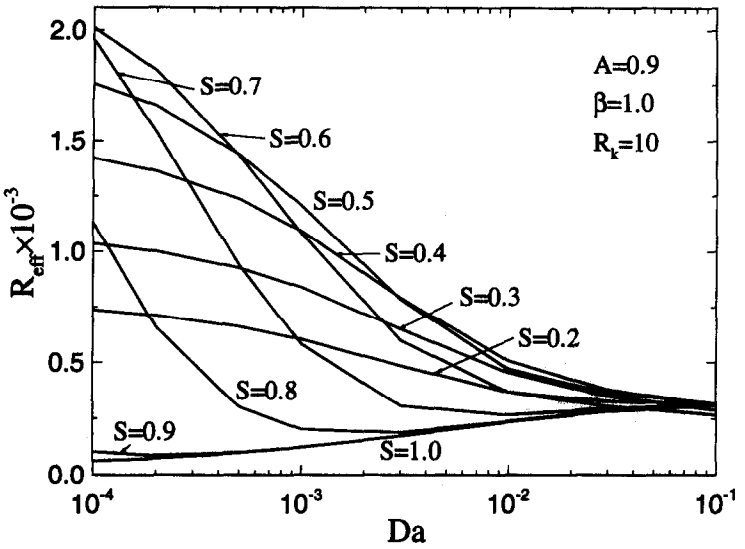

Fig. 8. R_{eff} vs Da for different thickness of porous layer. $A = 0.9$, $\beta = 1.0$, $Pr = 7.0$, $Re = 50$ and $R_k = 10$.

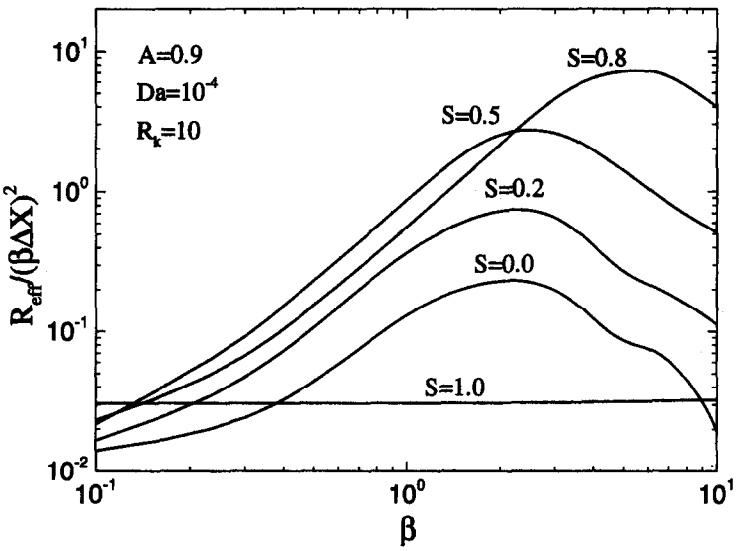

Fig. 9. Variations of $R_{\text{eff}}/(\beta\Delta X)^2$ against the frequency of pulsation. $A = 0.9$, $Da = 10^{-4}$. $Pr = 7.0$, $Re = 50$ and $R_k = 10$.

In the case of no porous medium ($S = 0.0$), Kurzweg and Zhao [12] analyzed that R_{eff} is proportional to $\beta\Delta X^2$, $(\beta\Delta X)^2$ and $(\beta^2\Delta X)^2$ when $\beta^2 Pr$ is high, moderate and low, respectively. If the ratio $R_{\text{eff}}/(\beta\Delta X)^2$ is employed as shown in Fig. 9, the above-stated three regions can be encompassed. Figure 9 depicts β and ΔX on heat transfer for various S at $Da = 10^{-4}$, $A = 0.9$, $Pr = 7.0$, $Re = 50$ and $R_k = 10$. It is observed that, in the limiting case ($S = 1.0$), R_{eff} is linearly proportional to $(\beta\Delta X)^2$. In the case of a pipe partially filled with porous medium ($S = 0.2, 0.5$ and 0.8) or no porous medium ($S = 0$), the dependence of $R_{\text{eff}}/(\beta\Delta X)^2$ on β is non-monotonic. $R_{\text{eff}}/(\beta\Delta X)^2$ increases as β increases up to a nearly constant value, which varies with S. This belongs to the region where R_{eff} is proportional to $(\beta^2\Delta X)^2$. After passing the region, i.e. $R_{\text{eff}}/(\beta\Delta X)^2$ is constant, $R_{\text{eff}}/(\beta\Delta X)^2$ decreases. The later region is equivalent to the case where R_{eff} is proportional to $\beta\Delta X^2$. Thus, an optimal frequency exists for achieving maximum $R_{\text{eff}}/(\beta\Delta X)^2$. These are qualitatively in identity with the results of Kurzweg and Zhao [12]. Physically, the optimal β means that there is sufficient time for heat to flow from the fluid core to the wall or before the temperature reverses itself within the core [11]. At the same time, the time-dependent gradient in the transverse direction remains large so as to allow a large heat flow in that direction. As expected, a different trajectory can be found for $S = 0.8$.

The effect of the amplitude of pulsation, for a fixed

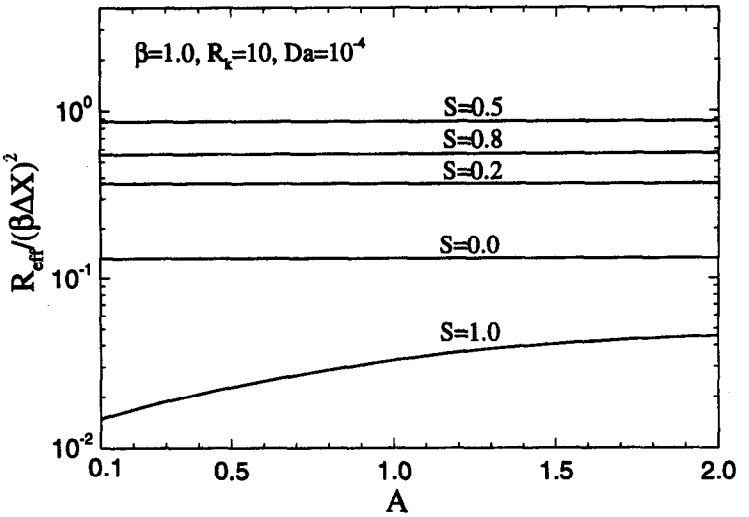

Fig. 10. Variations of $R_{eff}/(\beta\Delta X)^2$ against the amplitude of pulsation. $\beta = 1.0$, $Da = 10^{-4}$, $Pr = 7.0$, $Re = 50$ and $R_k = 10$.

frequency $\beta = 1.0$, is portrayed in Fig. 10 in the case of $Da = 10^{-4}$, $C_F = 0.057$, $Pr = 7.0$, $Re = 50$ and $R_k = 10$. As stated earlier, R_{eff} is linearly proportional to the square of the tidal displacement in the case of no porous medium. This means that $R_{eff}/(\beta\Delta X)^2$ remains constant while the amplitude A varies. The limiting case for $S = 0.0$ in Fig. 10 is fully consistent with the above-analysis. Of interest is that R_{eff} is still linearly proportional to $\Delta X^2(\beta = 1.0)$ in a composite system ($S = 0.2$, 0.5 and 0.8). This is because the porous region has little contribution to the tidal displacement. In the case of $S = 1.0$, $R_{eff}/(\beta\Delta X)^2$ increases as A increases.

5. CONCLUSION

Detailed numerical analyses were performed to delineate the pulsating flow and heat transfer characteristics in a circular pipe partially filled with a porous medium. The main emphasis was placed on the minimization of the mechanical loss due to pressure drop as well as the enhancement of heat transfer by partial filling of porous media. The computed results were shown to be in close agreement with available analyses. The maximum effective thermal diffusivity was achieved by pulsating flow through a pipe partially filled with porous material rather than the limiting cases of no porous medium or the full filling of a porous material. An optimal porous layer thickness (S) was obtained by plotting the ratio of the effective thermal diffusivity (R_{eff}), which depends on Da. Parameter studies revealed that, as Da increases, the dependence of R_{eff} on S weakens considerably. As S increases further, a different trend emerges on the R_{eff} distribution. In particular, the dependence of R_{eff} on Da is marginal for $S \approx 0.8$. The effect of pulsation on heat transfer was represented by the tidal displacement (ΔX) and a function of β, i.e. $R_{eff}/(\beta\Delta X)^2$. It was also found that an optimal β exists for achieving the maximum $R_{eff}(\beta\Delta X)^2$, which varies with S. In addition, for high conducting porous media ($R_k = 100$), Nu increases monotonically with increasing S. However, for a lower value of R_k ($R_k = 1$), a minimum exists in the Nu distribution via S.

REFERENCES

1. Vafai, K. and Tien, C. L., Boundary and inertia effects on flow and heat transfer in porous media. *International Journal of Heat and Mass Transfer*, 1981, **24**, 195–203.
2. Kaviany, M., Laminar flow through a porous channel bounded by isothermal parallel plates. *International Journal of Heat and Mass Transfer*, 1985, **28**, 851–858.
3. Hunt, M. L. and Tien, C. L., Effects of thermal dispersion on forced convection in fibrous media. *International Journal of Heat and Mass Transfer*, 1988, **31**, 301–309.
4. Lauriat, G. and Vafai, K., Forced convective flow and heat transfer through a porous medium exposed to a flat plate or a channel. In *Convective Heat and Mass Transfer in Porous Media*, NATO ASI Series, Series E: Vol. 196. Kluwer Academic Publishers, 1991, pp. 289–327.
5. Tong, T. W. and Sharatchandra, M. C., Heat transfer enhancement using porous inserts. *Heat Transfer and Flow in Porous Media*, HTD 156. 1990, pp. 41–46.
6. Poulikakos, D. and Kazmierczak, M., Forced convection in a duct partially filled with a porous material. *Trans. ASME Journal of Heat Transfer*, 199=87, **109**, 653–662.
7. Chikh, S., Boumedien, A., Bouhadef, K. and Lauriat, G., Analytical solution of non-Darcian forced convection in an annular duct partially filled with a porous medium. *International Journal of Heat and Mass Transfer*, 1995, **38**, 1543–1551.
8. Sung, H. J., Kim, S. Y. and Hyun, J. M., Forced convection from an isolated heat source in a channel with porous medium. *International Journal of Heat and Fluid Flow*, 1995, **16**, 527–535.
9. Chatwin, P. C., On the longitudinal dispersion of passive contaminant in oscillatory flows in tubes. *Journal of Fluid Mechanics*, 1975, **71**, 513–527.
10. Watson, E. J., Diffusion in oscillatory pipe flow. *Journal of Fluid Mechanics*, 1983, **133**, 233–244.
11. Kurzweg, U. H., Enhanced heat conduction in oscillatory viscous flows within parallel-plate channels. *Journal of Fluid Mechanics*, 1985, **156**, 291–300.

12. Kurzweg, U. H. and Zhao, L. D., Heat transfer by high frequency oscillations: a new hydrodynamic technique for achieving large effective thermal conductivities. *Physics of Fluid*, 1984, **27**, 2624–2627.
13. Simon, T. W. and Seume, J. R., A survey of oscillating flow in stirling engine heat exchangers. NASA Contractor Report 182108, 1988.
14. Kim, S. Y., Kang, B. H. and Hyun, J. M., Heat transfer from pulsating flow in a channel filled with porous media. *International Journal of Heat and Mass Transfer*, 1994, **37**, 2025–2033.
15. Khodadadi, J. M., Oscillatory fluid flow through a porous medium channel bounded by two impermeable parallel plates. *Journal of Fluid Engineering*, 1991, **113**, 509–511.
16. Patankar, S. V., *Numerical Heat Transfer and Fluid Flow*. Hemisphere, New York, 1980, p. 30.
17. Hadim, A., Forced convection in a porous channel with localized heat sources. *Transactions of ASME Journal of Heat Transfer*, 1994, **116**, 465–472.
18. Huang, P. C. and Vafai, K., Analysis of flow and heat transfer over an external boundary covered with a porous substrate. *Transactions of ASME Journal of Heat Transfer*, 1994, **116**, 768–771.
19. Lundgren, T. S., Slow flow through stationary random beds and suspension of spheres. *Journal of Fluid Mechanics*, 1972, **51**, 273–299.
20. Uchida, S., The pulsating viscous flow superposed on the steady laminar motion of incompressible fluid in a circular pipe. *ZAMP*, 1956, **7**, 403–422.
21. Cho, H. W. and Hyun, J. M., Numerical solutions of pulsating flow and heat transfer characteristics in a pipe. *International Journal of Heat and Fluid Flow*, 1990, **11**(4), 321–330.
22. Siegel, R. and Perlmutter, M., Heat transfer for pulsating laminar duct flow. *Transactions ASME Journal of Heat Transfer*, 1962, **84**(2), 111–123.
23. Siegel, R., Influence of oscillation-induced diffusion on heat transfer in a uniformly heated channel. *Transactions of ASME Journal of Heat Transfer*, 1987, **109**, 224–247.
24. Valueva, E. P., Popov, V. N. and Romanova, S. Yu., Heat transfer under laminar pulsating flow in a round tube. *Thermal Engineering*, 1993, **40**, 624–631.